

## **TRIBOLOGICAL PROPERTIES**

---

### **4.1 Introduction**

Tribological properties of the materials are affected by many parameters. Present chapter deals with the studies and discussion on the effect of sliding distance, sliding velocity, applied normal load, and vol. % of ZrB<sub>2</sub> particles on wear and friction properties of the composites. Wear and friction have been studied at ambient temperature under dry sliding conditions for all compositions. Worn surfaces have been studied under SEM and profilometer to analyse wear results. Energy dispersive spectroscopy of worn surfaces and wear debris is also conducted for better understanding of the operative wear mechanism.

### **4.2 Wear and Friction Study**

Following subsections present the effect of sliding distance, sliding velocity, normal load and vol. % of ZrB<sub>2</sub> particles on wear and friction properties of the composites.

#### **4.2.1 Effect of Sliding Distance**

Figure 4.1a-d presents the variation of cumulative wear loss of base alloy and composites as a function of sliding distance at different loads (10 - 40 N) and 1 m/s

sliding velocity. It is observed that wear loss increases with increase in the sliding distance for all composites and base alloy. All composites and base alloy show a linear increase in cumulative wear with distance. However, a decrease in wear loss is observed with increasing vol. % of  $ZrB_2$  particles due to increase in hardness.

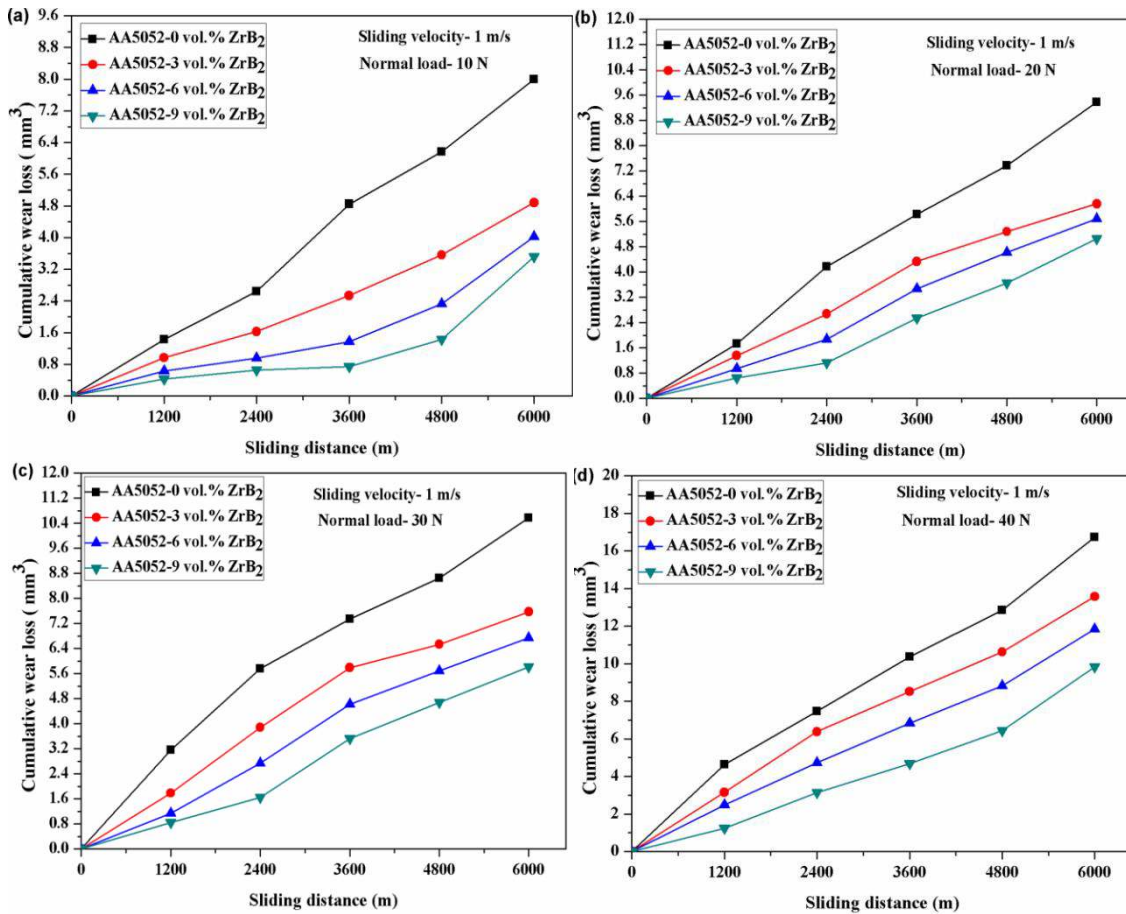


**Figure 4.1** - Variation of cumulative wear with sliding distance at (a) 10 N (b) 20 N (c) 30 N and (d) 40 N and 1 m/s sliding velocity

Coefficient of friction fluctuates within a range of  $\pm 0.025$  for all compositions with sliding distance (Fig. 4.2 a-d). COF of composites is higher than that of base alloy while sliding under identical conditions at different loads (10 to 40 N). The higher coefficient of friction in the composites is due to the presence of hard particles at the interface between two contacting surfaces. With increasing amount of  $ZrB_2$  particles, direct contact of hard steel disc with softer matrix phase of the composites gets minimised

which causes wear rate to decrease, while the hard  $ZrB_2$  particles counteract with hard steel surface and an increase in COF is observed due to these hard particles [Kumar et al., 2015c; 2016a].

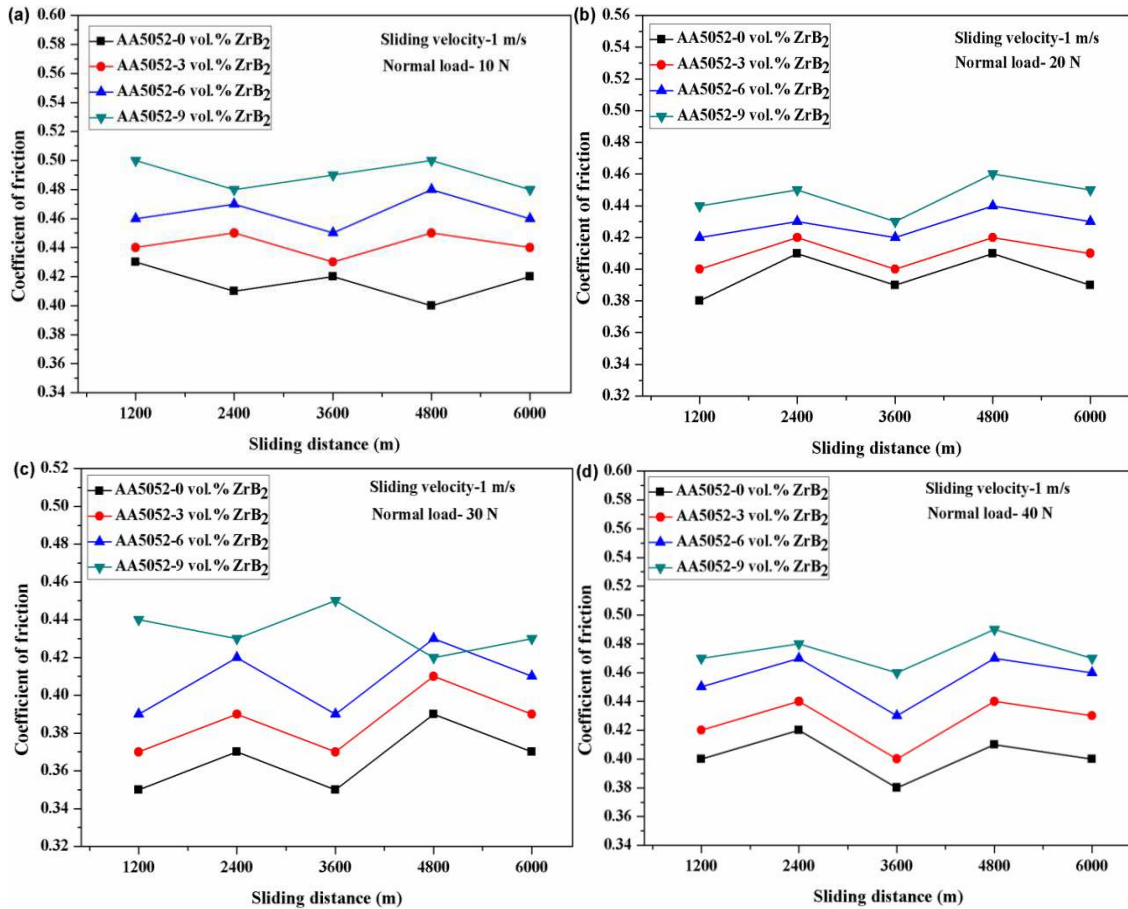


**Figure 4.2** - Variation of COF with sliding distance at (a) 10 N (b) 20 N (c) 30 N and (d) 40 N and 1 m/s sliding velocity

#### 4.2.2 Effect of Sliding Velocity

Figure 4.3a-d shows the effect of sliding velocity on wear rate of as cast AA5052 alloy and composites at different loads 10-40 N. It is evident from the figures that wear rate continuously increases with an increase in sliding velocity for all compositions. When the pin sample and disc surfaces are in relative sliding contact under normal load, frictional heating occurs between two surfaces. The heat generated depends on the sliding velocity [Rao and Das, 2011]. Due to softening of the surface, hard particles

(ZrB<sub>2</sub> or Al<sub>2</sub>O<sub>3</sub>) may come out of the surface and may cause third body wear. Hence, the nature of wear changes from mild to severe, thereby increasing the overall wear. It is also likely that hard asperities of steel surface may also penetrate through the soft surface increasing the wear rate [Kumar et al., 2016a].

Sliding velocity also affects the coefficient of friction and it increases with an increase in sliding velocity (Fig. 4.4a-d), which could be due to the increased rate of oxidation, removal of oxide particles from the surfaces and increase in external particle contribution ( $\mu_{part}$ ). The contribution of  $\mu_{part}$  dominates and enhances the overall coefficient of friction. It is reported that at higher velocities temperature of mating surfaces leads to more asperities at the junctions resulting in higher coefficient of friction [Kumar et al., 2016a; Ramesh and Ahamed, 2011; Rana and Stefanescu, 1989].

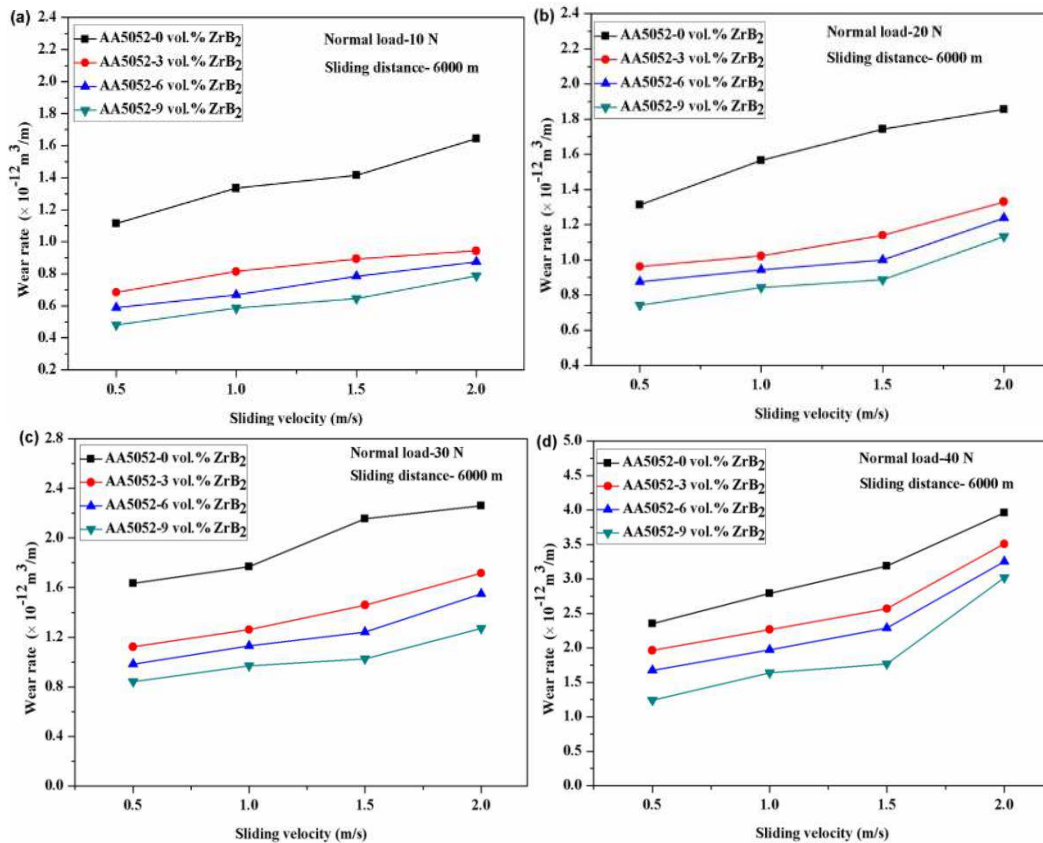


Figure 4.3 - Variation of wear rate with sliding velocity at (a) 10 N (b) 20 N (c) 30 N and (d) 40 N load

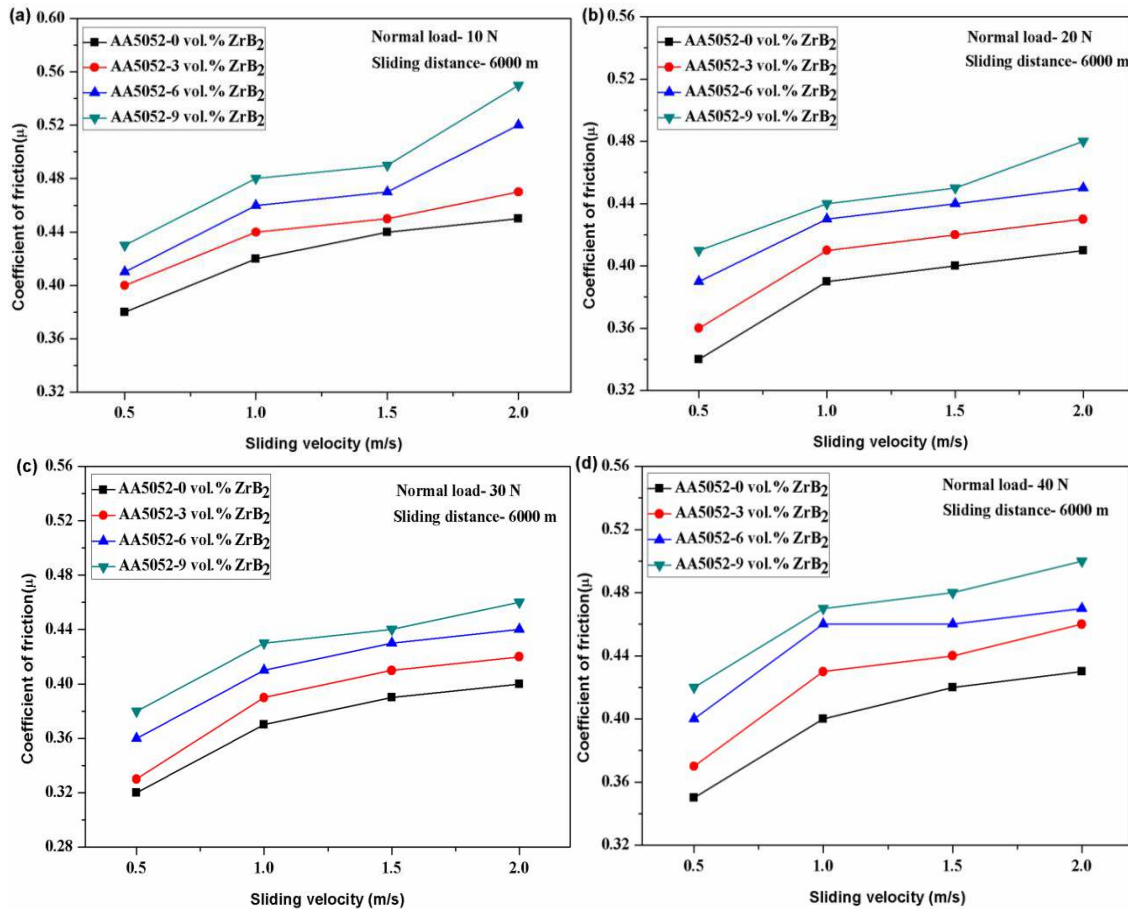
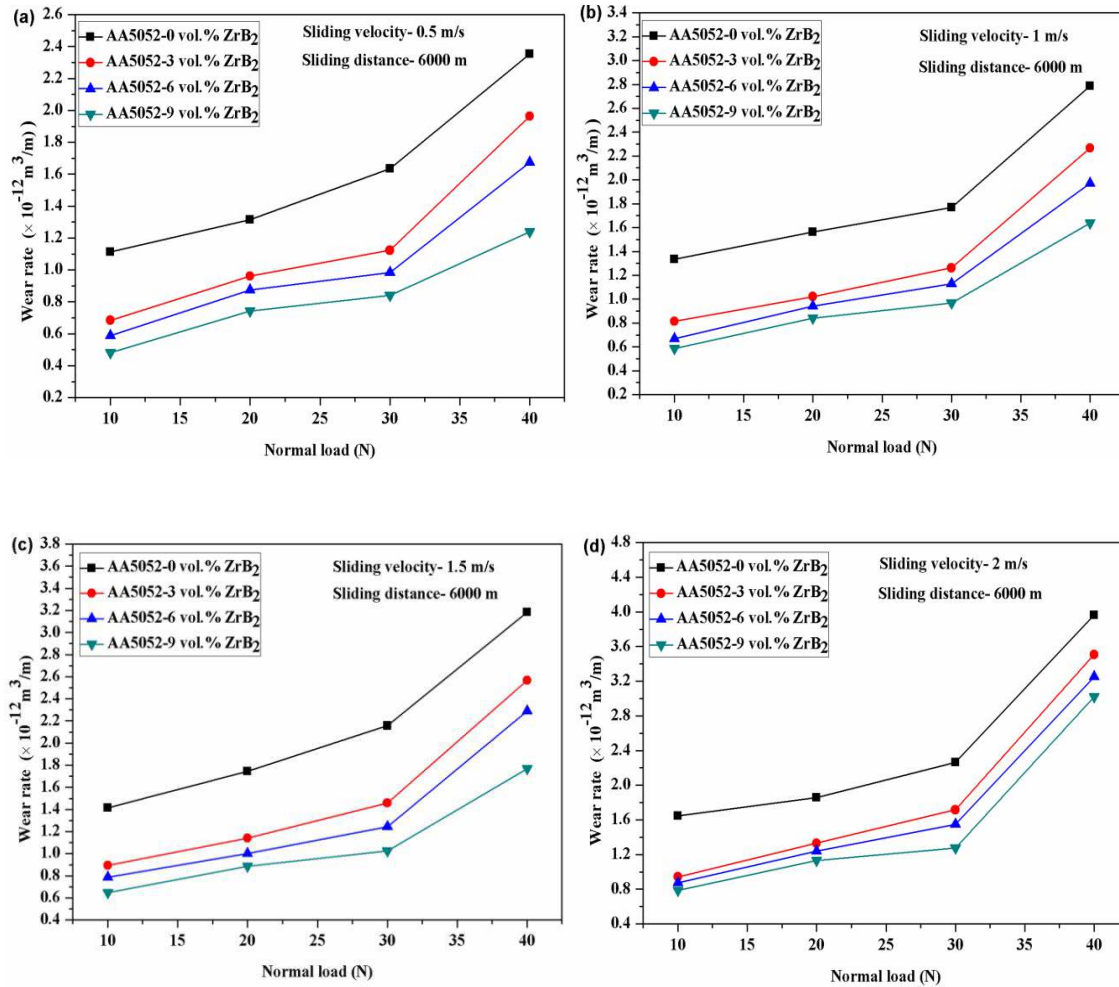


Figure 4.4 - Variation of COF with sliding velocity at (a) 10 N (b) 20 N (c) 30 N and (d) 40 N load

### 4.2.3 Effect of Normal Load

It is clear from Fig.4.5a-d that the wear rate increases with an increase in normal load for as cast AA5052 alloy and composites at different sliding velocities from 0.5 to 2 m/s. With an increase in load counteracting hard asperities may lead to ploughing and delamination of surface creating large grooves in the surface which lead to high wear rate. Further, increase in load may also cause micro-cracking at subsurface level. Asperities may be either removed from the surface or deformed in the sub-surface. In the presence of hard ZrB<sub>2</sub> particles a mechanically mixed layer (MML) of soft aluminium base matrix and hard particles of ZrB<sub>2</sub> is formed. This MML restricts the transfer of material from the surface and wear remains in mild wear regime and

dominated by oxidative mode with reduced wear rate. But beyond 30N load, cracking of this MML takes place and hard  $ZrB_2$  particles come out of MML and act as third body abrasion and transition from mild/oxidative to severe/oxidative-metallic wear takes place enhancing the wear rate as shown in Fig 4.5a-d (sharp increase in wear rate beyond 30 N) [Kumar et al., 2015c; 2016a].



**Figure 4.5** - Variation of wear rate with normal load at (a) 0.5 (b) 1 (c) 1.5 and (d) 2 m/s sliding velocity

Effect of *insitu* formed  $ZrB_2$  particles becomes further evident from Fig. 4.6a-d which shows the variation of wear rate per unit vol. %  $ZrB_2$  as a function of applied normal load for different compositions at different sliding velocities from 0.5 to 2 m/s. This parameter gives an indirect measure of load bearing capacity of composite [Natarajan et

al., 2009]. It should also be noted that beyond 3 vol. %  $ZrB_2$  this parameter decreases drastically which may be attributed to the decrease in Al-rich phase cell size at higher vol. % of  $ZrB_2$  particles [Mandal et al., 2004]. However, coefficient of friction decreases initially (Fig. 4.7a-d) with an increase in load up to 30 N due to the formation of MML providing a smooth surface, but beyond 30 N load, cracking in MML takes place and hard particles come in direct contact with secondary surface and the coefficient of friction increases sharply [Kumar et al., 2016a].

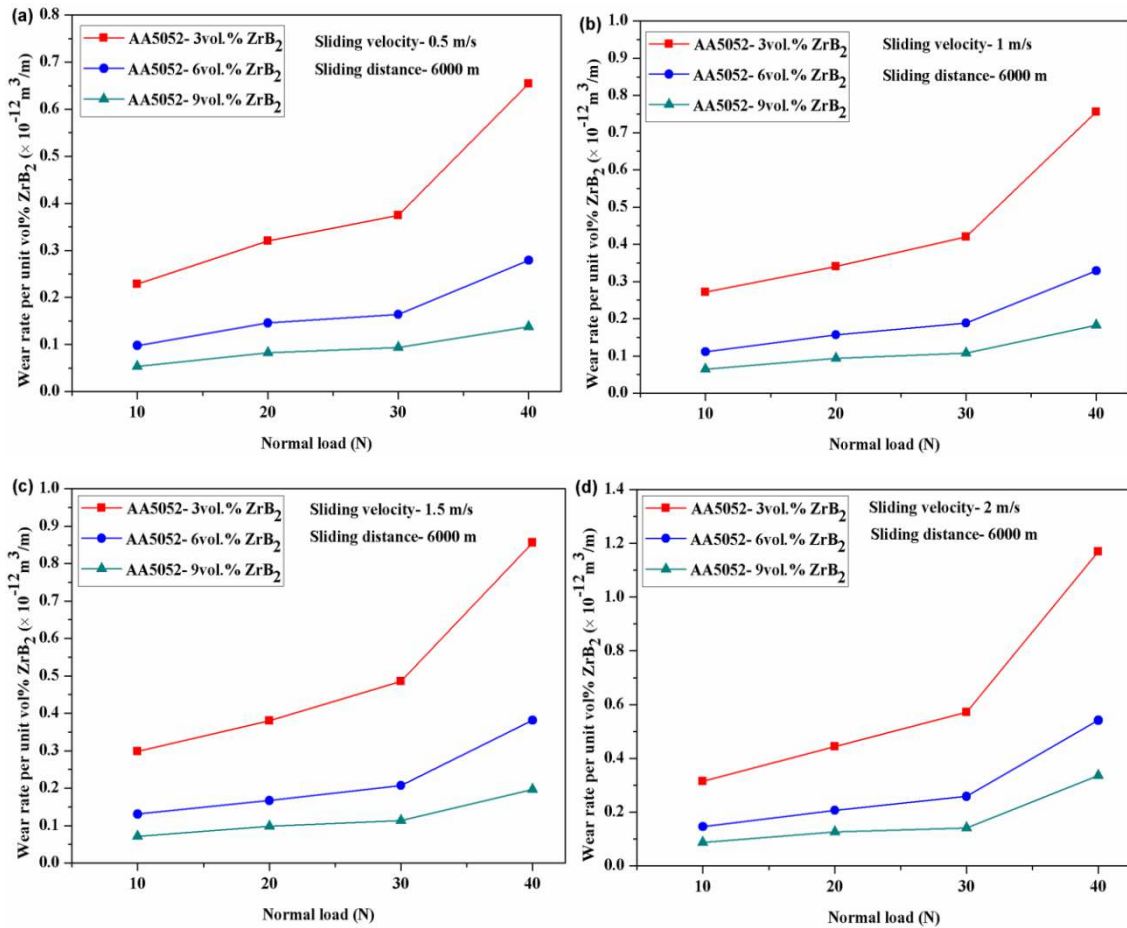


**Figure 4.6** - Variation of wear rate per unit vol. %  $ZrB_2$  with normal load at (a) 0.5 (b) 1 (c) 1.5 and (d) 2 m/s sliding velocity

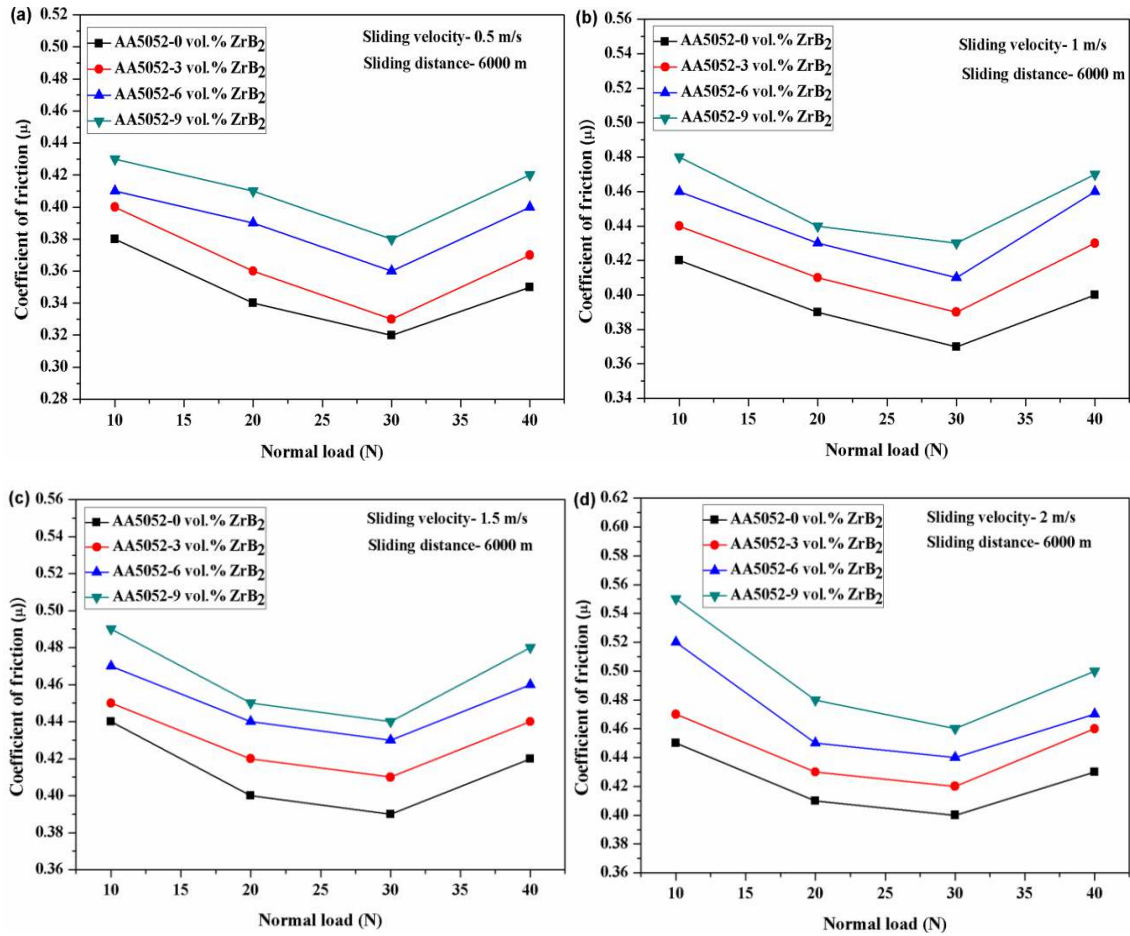
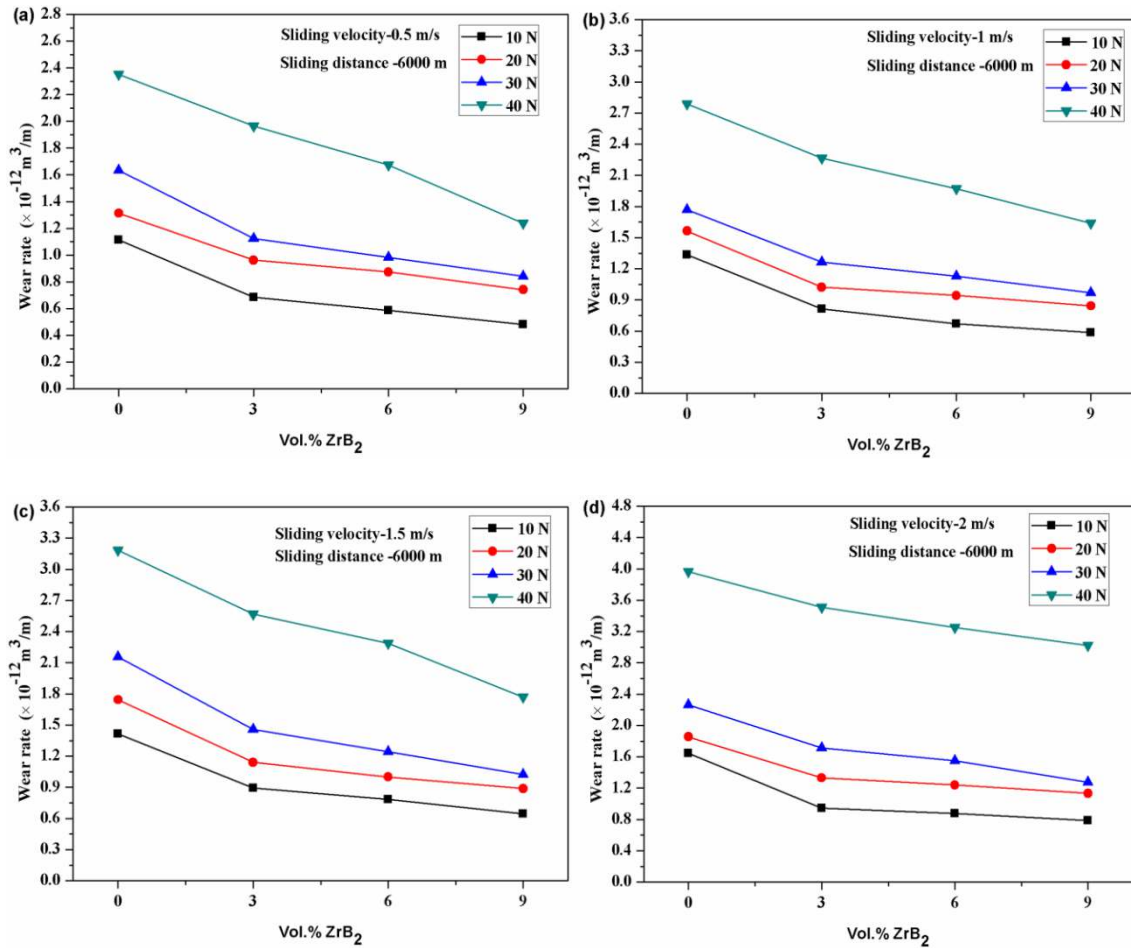


Figure 4.7 - Variation of COF with normal load at (a) 0.5 (b) 1 (c) 1.5 and (d) 2 m/s sliding velocity

#### 4.2.4 Effect of vol. % of ZrB<sub>2</sub> Particles

Wear rate, specific wear rate (wear rate per unit load) and normalized wear rate (wear rate of composite normalised with respect to wear rate of base alloy) of AA5052 alloy and composites decrease with an increase in vol. % of ZrB<sub>2</sub> particles at different sliding velocities and applied loads as shown from the Figs. 4.8a-d to 4.10a-d. MML restricts the removal of material from the surface and with an increase in the vol. % of ZrB<sub>2</sub> in MML the hardness of the composite increases which helps in decreasing the wear rate which is in agreement with Archard's wear law [Archard, 1953].



**Figure 4.8** - Variation of wear rate with vol. %  $\text{ZrB}_2$  at (a) 0.5 (b) 1 (c) 1.5 and (d) 2 m/s sliding velocity

Grain refinement, good interfacial bonding and increased dislocation density due to increase in vol. % of  $\text{ZrB}_2$  particles lead to enhanced hardness and strength of the composites which contribute to lowering of wear rate [Gupta and Srivatsan, 2001]. Further,  $\text{ZrB}_2$  particles also reduce the extent of direct metal-to-metal contact between matrix and counter face and that also improves the load bearing capacity of the composites during sliding process [Kumar et al., 2015c; 2016a].

Figure 4.11a-d shows the variation of coefficient of friction with  $\text{ZrB}_2$  content at different loads (10 to 40 N) for all sliding velocities (0.5, 1, 1.5 & 2 m/s) used in the present study. It is observed that coefficient of friction increases with an increase in the vol. %  $\text{ZrB}_2$  particles. With an increase in the amount of  $\text{ZrB}_2$  particles in the MML,

coefficient of friction increases as a result of increased amount of large abrasive particles, while, other factors contributing to friction remain more or less same, and a continuous increase in coefficient of friction is observed [Kumar et al., 2015c; 2016a].

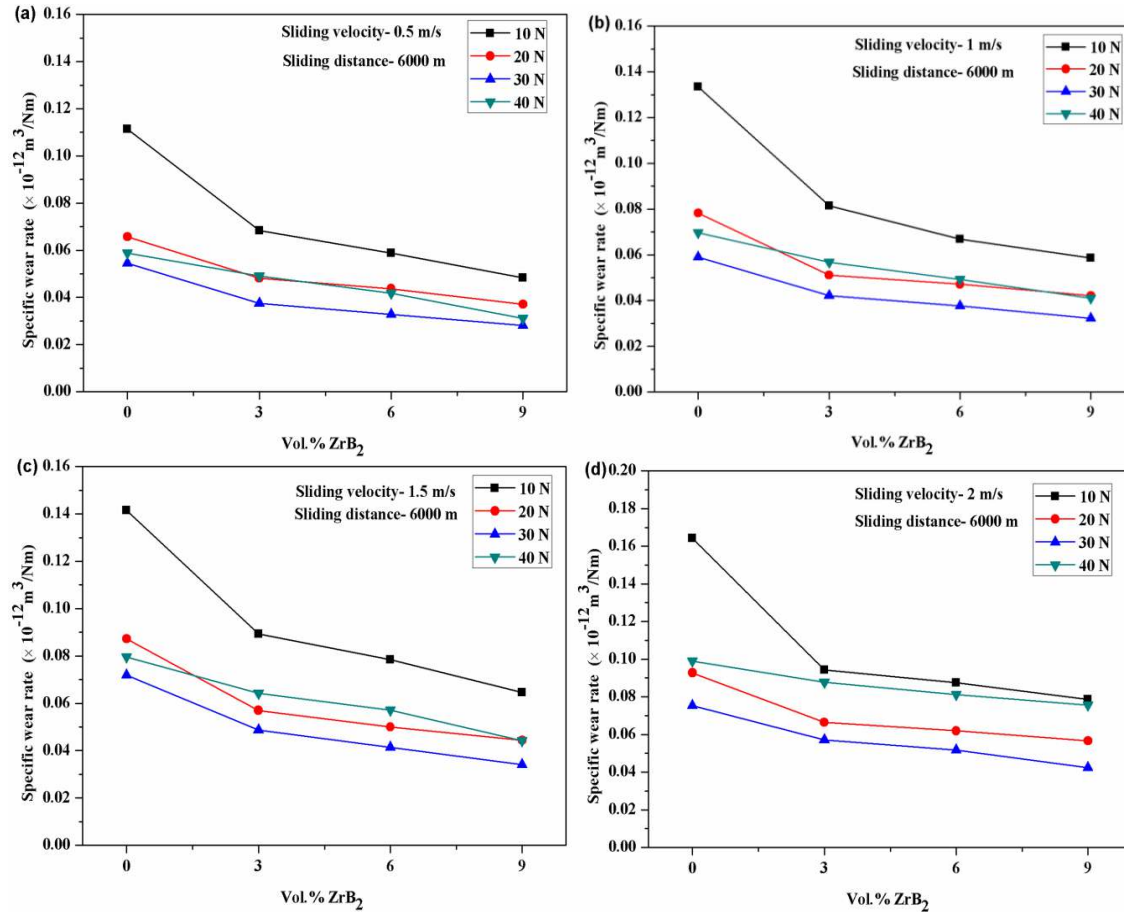


**Figure 4.9** - Variation of specific wear rate with vol. %  $\text{ZrB}_2$  at (a) 0.5 (b) 1 (c) 1.5 and (d) 2 m/s sliding velocity

### 4.3 Wear Mechanism and Worn Surface Analysis

To understand the wear mechanism, it is important to study the wear debris and worn surfaces; therefore, a detailed study of worn surfaces at different parameters has been conducted under SEM and Profilometer. Figure 4.12a-b shows the SEM micrographs of the worn surfaces of 9 vol. %  $\text{ZrB}_2$  composite after 1200 m and 6000 m sliding distance at 0.5 m/s sliding velocity and 10 N normal load. Figure 4.12a reveals the shallow ploughing marks and grooves, but no delamination and cracks are seen at 1200 m. But

in Fig. 4.12b deep ploughing and grooves with large amount of delamination and cracks are clearly visible after 6000 m sliding distance. Contour of worn surface shows the different level of surface roughness and their roughness profile is also shown in Fig.4.13a-b. These profiles clearly indicate the variation of surface roughness from valley to peaks and an average line is drawn in contour to see the nature of profile on that particular line. 3D topography of worn surface also shows the shallow grooves after 1200 m, the grooves are deeper after 6000 m sliding distance. The surface roughness corresponding to 1200 m and 6000 m sliding distance are 3.30 and 4.44  $\mu\text{m}$ .

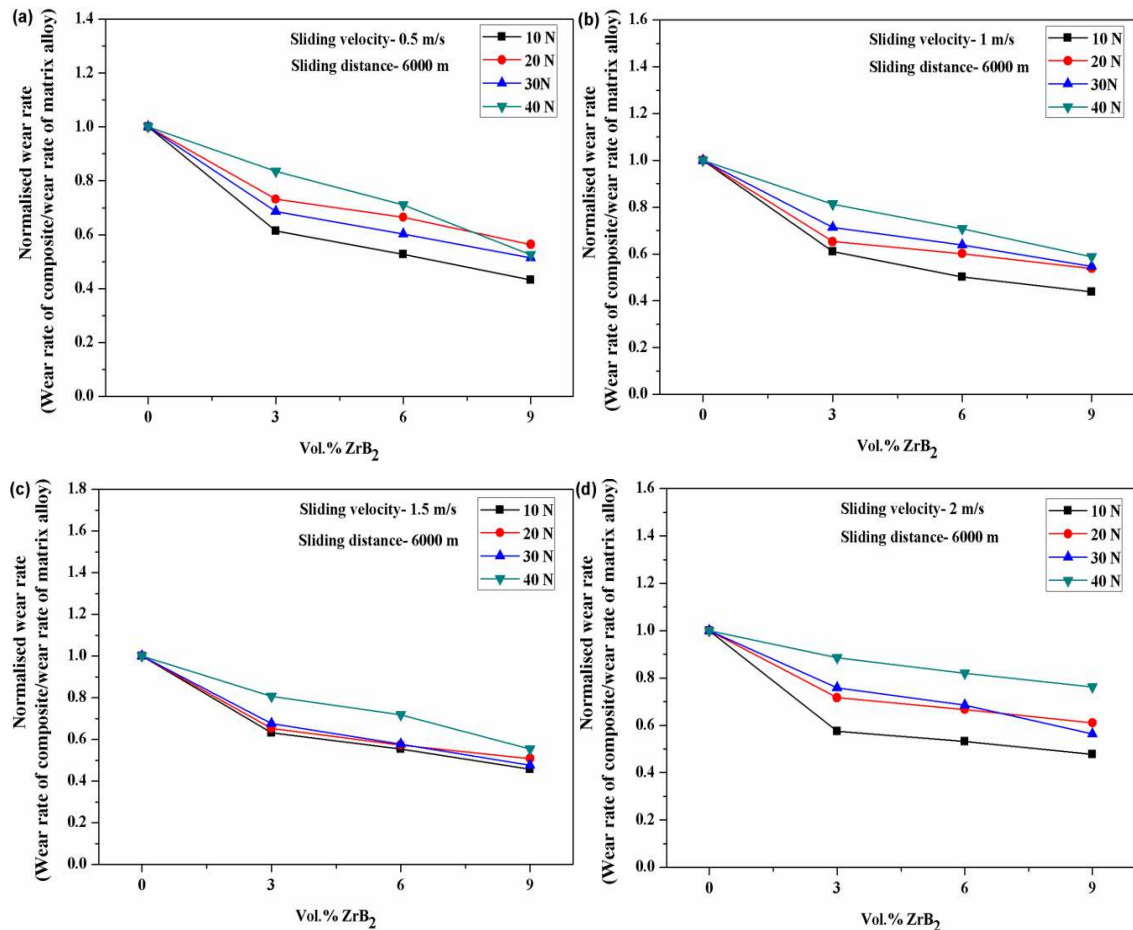


**Figure 4.10** - Variation of normalised wear rate with vol. % ZrB<sub>2</sub> at (a) 0.5 (b) 1 (c) 1.5 and (d) 2 m/s sliding velocity

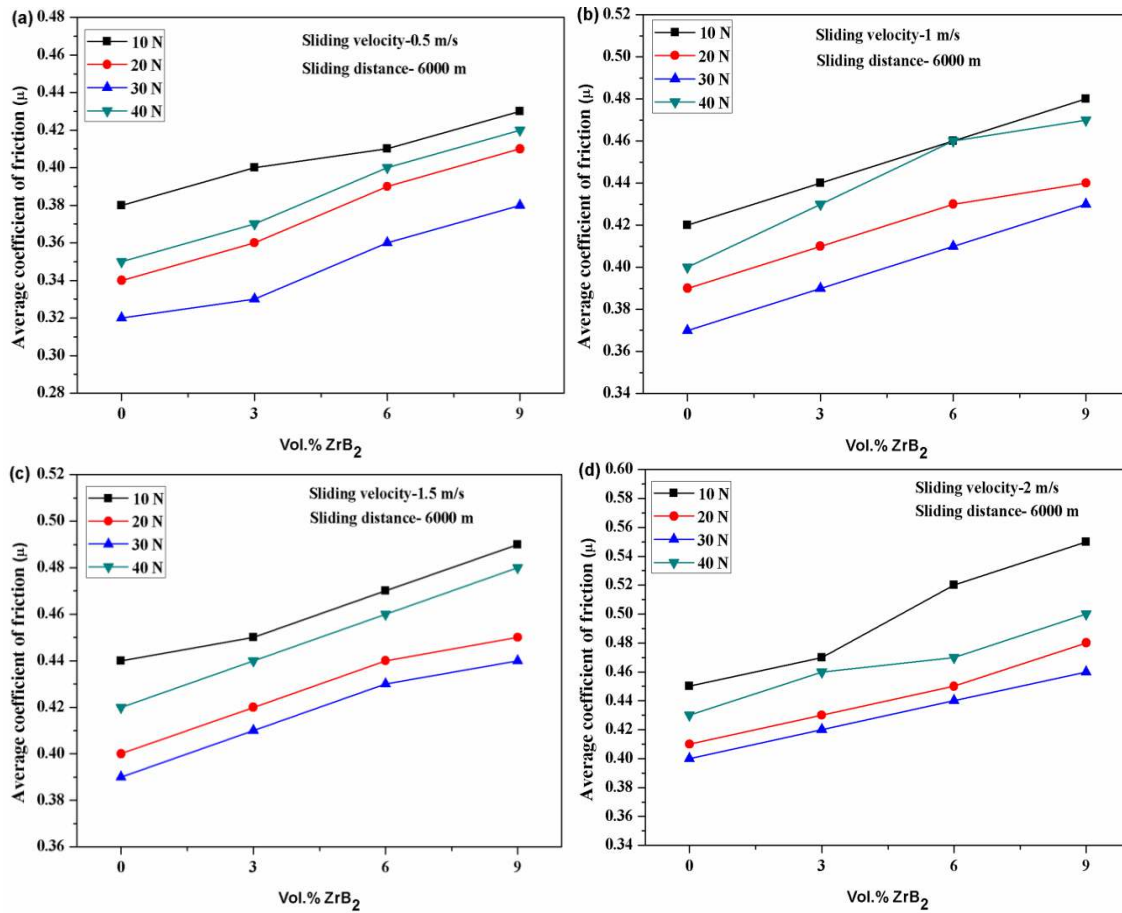


Figure 4.11 - Variation of COF with vol. %  $ZrB_2$  at (a) 0.5 (b) 1 (c) 1.5 and (d) 2 m/s sliding velocity

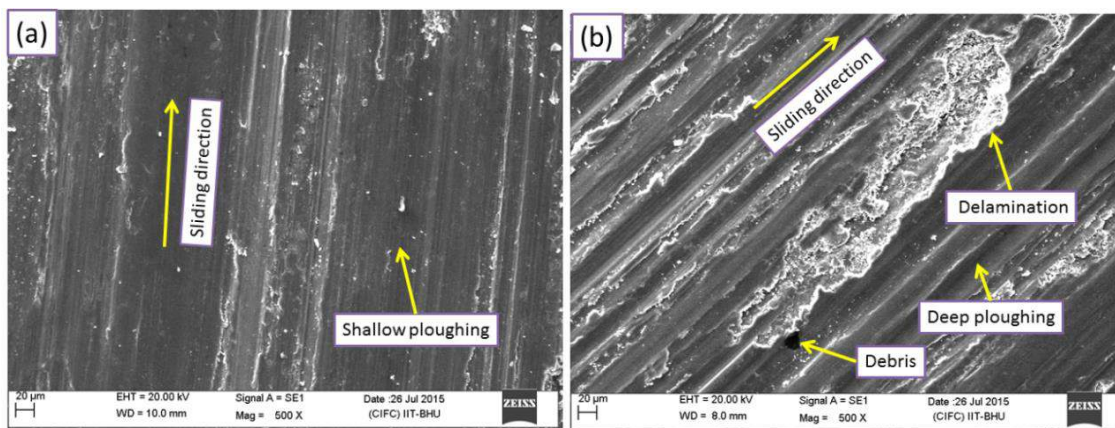
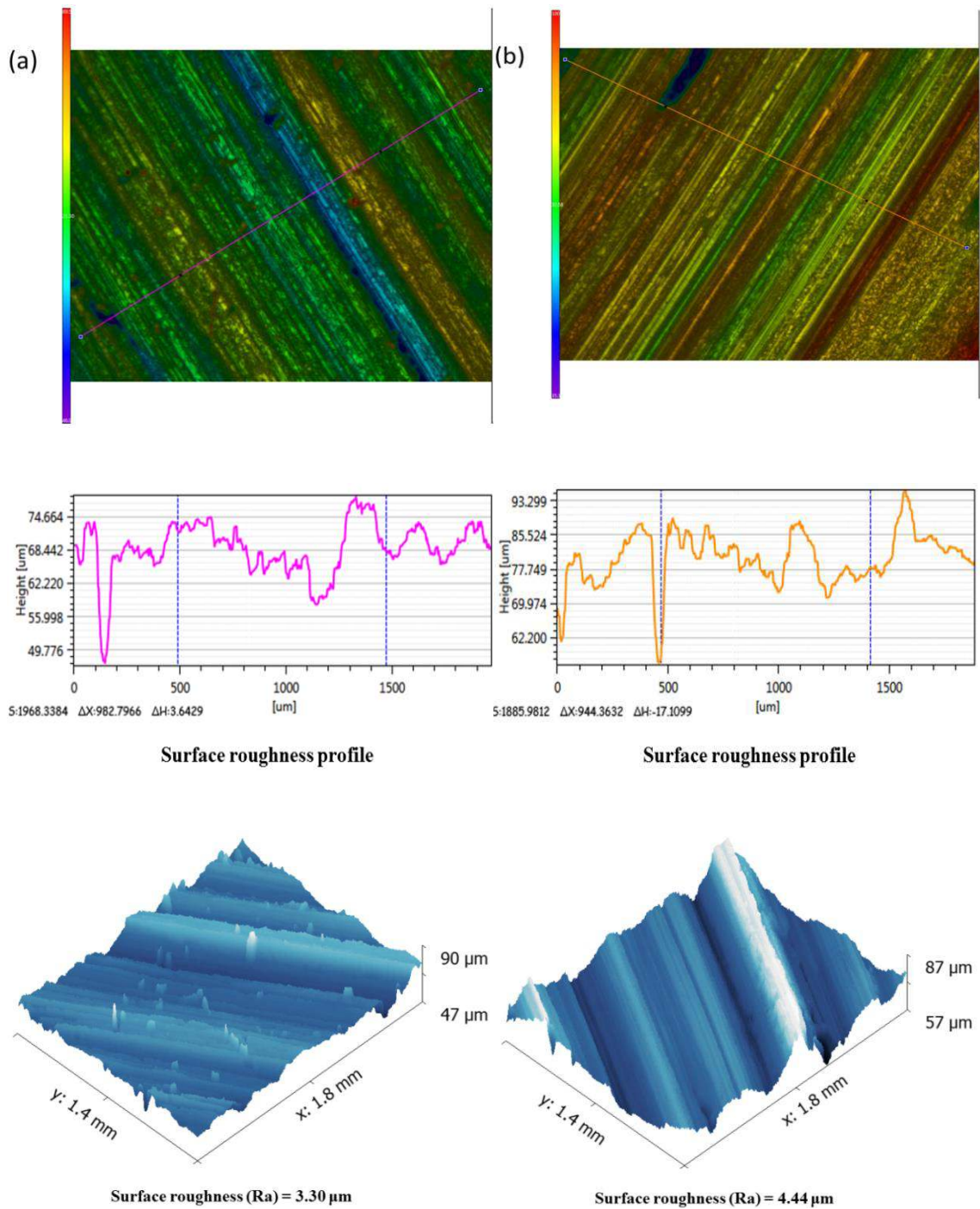


Figure 4.12 - Worn surface morphology of 9 vol. %  $ZrB_2$  composite after (a) 1200 m and (b) 6000 m sliding distance



**Figure 4.13** - 2D and 3D topography of worn surface of 9 vol. % ZrB<sub>2</sub> composite after (a) 1200 m and (b) 6000 m sliding distance under profilometer

Figure 4.14a-d shows the worn surface topography of 9 vol. % ZrB<sub>2</sub> composite at different sliding velocities (0.5, 1, 1.5 & 2 m/s) and 20 N normal load. Figure 4.14a shows the smooth surface with shallow grooves (indicative of mild wear), and less

amount of delamination which may be due to less frictional heating between the counter surfaces at 0.5 m/s. Depth of groove and delamination increases with sliding velocity (Fig. 14b-d). Fig. 4.14d corresponds to 2 m/s sliding velocity where grooves are deep and large amount of delamination and cracks are seen (indicative of severe wear). The reason is that at higher sliding velocity the large amount of frictional heat is generated that leads to higher wear rate. Fig. 4.15a shows the EDS pattern of the worn surface of 9 vol. % composite at 0.5 m/s which consists of Al, O and Fe peaks which indicates oxidative wear. EDS pattern in Fig. 4.15b shows the peaks of elements Al, O, Fe, C and Zr which indicates that at higher sliding velocity of 2 m/s the wear is oxidative-metallic.

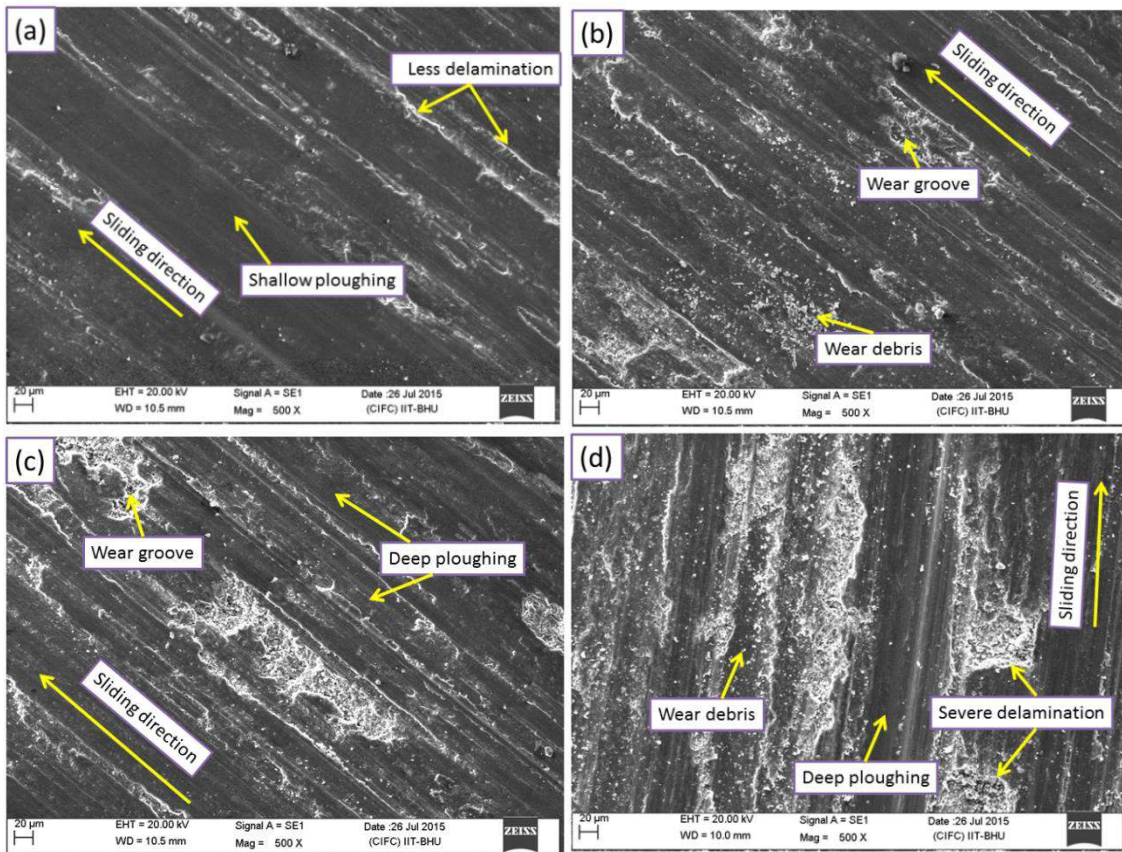


**Figure 4.14** - Worn surface morphology of 9 vol. %  $ZrB_2$  composite at (a) 0.5 (b) 1 (c) 1.5 and (d) 2 m/s at 20 N load and 6000 m sliding distance

Contour of worn surfaces and their roughness profile are also shown in Fig. 4.16a-b. These profiles clearly show the variation of surface roughness from valley to peaks and an average line is drawn in contour to see the nature of profile on that particular line. 3D topography of worn surfaces show the shallow grooves at 0.5 m/s sliding velocity and deep grooves at 2 m/s which result in the increased surface roughness.

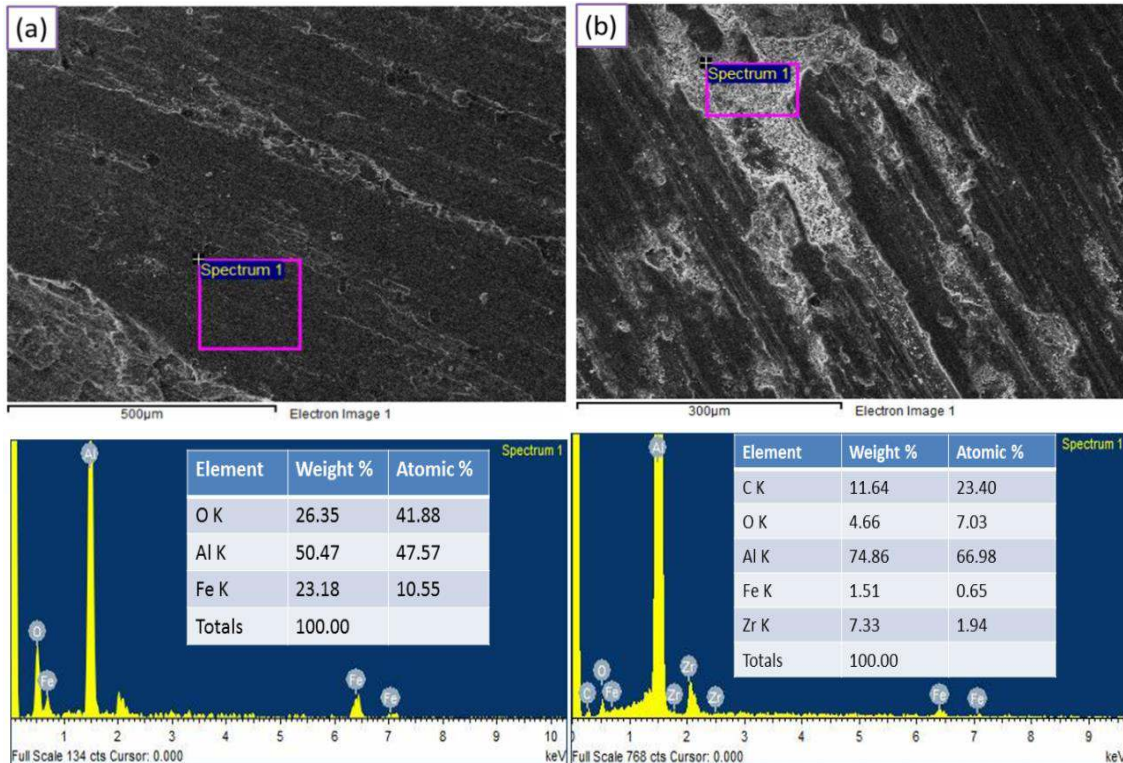


**Figure 4.15** - EDS pattern of 9 vol. % ZrB<sub>2</sub> composite at (a) 0.5 and (b) 2 under 20 N load and 6000 m sliding distance

Figure 4.17a-d shows the worn surface topography of 9 vol. % ZrB<sub>2</sub> composite at different loads 10 - 40 N keeping the sliding velocity at 1 m/s. Figure 4.17a exhibits relatively smooth surface with shallow grooves along with micro-ploughing of counter surface on the pin (mild wear regime) at 10 N load. Surface damage increases with load, and at 40 N worn surface is severely damaged and exhibits deep grooves, high plastic deformation at the edges and large number of cracks (severe wear regime) as

shown in Fig.4.17d. This leads to increase in wear rate. Figure 4.18a-b shows the different level of surface roughness of worn surfaces and their roughness profile is also shown in the figures. These profiles indicate the variation of surface roughness from valley to peaks and an average line is drawn in contour to see the nature of profile on that line.

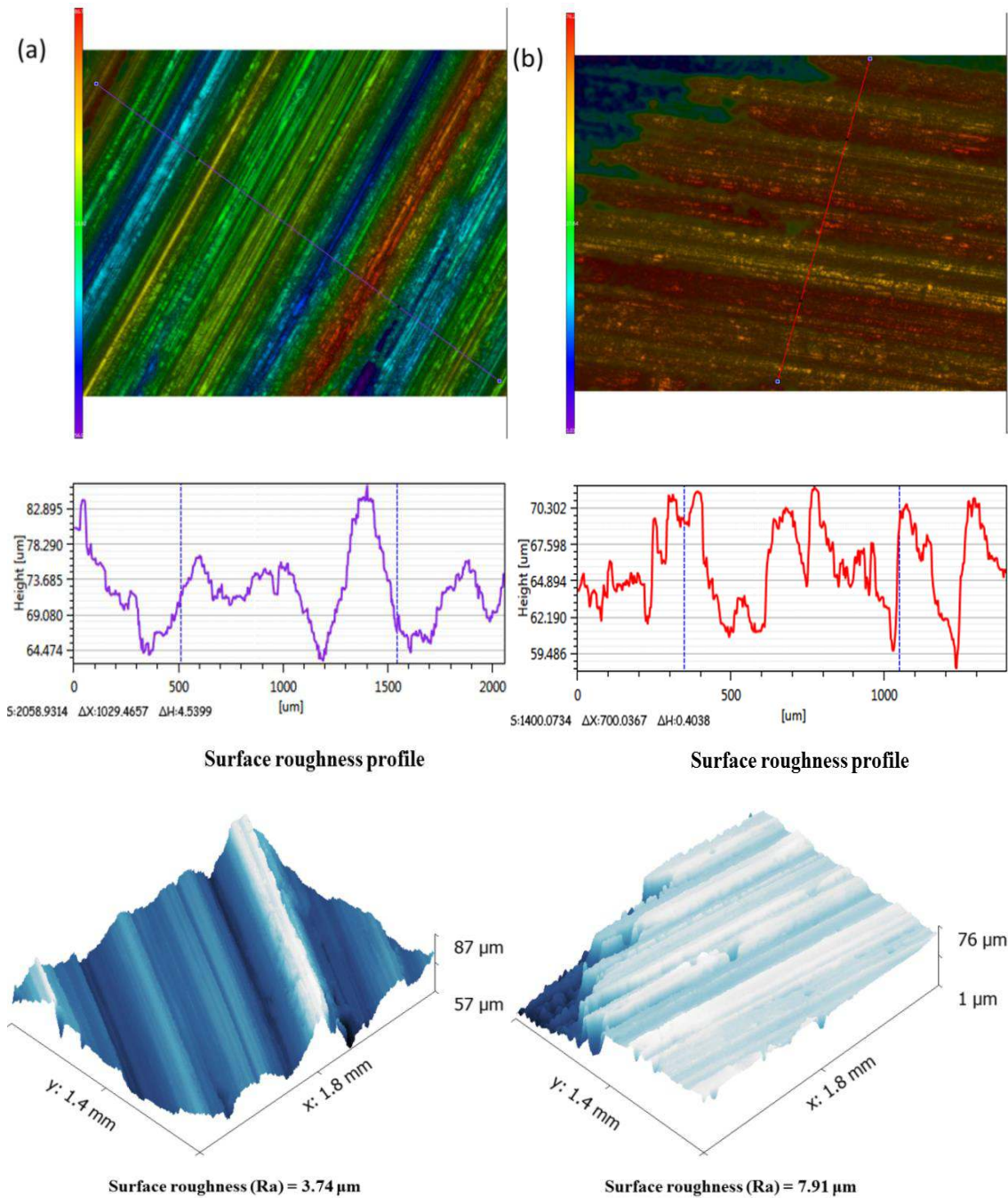


**Figure 4.16** - 2D and 3D topography of worn surface of 9 vol. % ZrB<sub>2</sub> composite at (a) 0.5 m/s and (b) 2 m/s sliding velocity and 20 N load after 6000 m sliding distance under profilometer

3D topography of worn surface also shows the shallow grooves at 10 N load and severely damaged surface with deep grooves and cracks at 40 N load indicative of highly rough surface. Further, EDS patterns of worn surface of 9 vol. % ZrB<sub>2</sub> composite are shown in Fig.4.19a-b which indicate the mild/oxidative wear at low load (10 N) and severe/oxidative-metallic wear at high load (40 N). EDS pattern of wear debris particles shown in Fig. 4.19c also indicates the presence of ZrB<sub>2</sub> particles in wear debris which act as third body abrasion giving rise to severe wear.

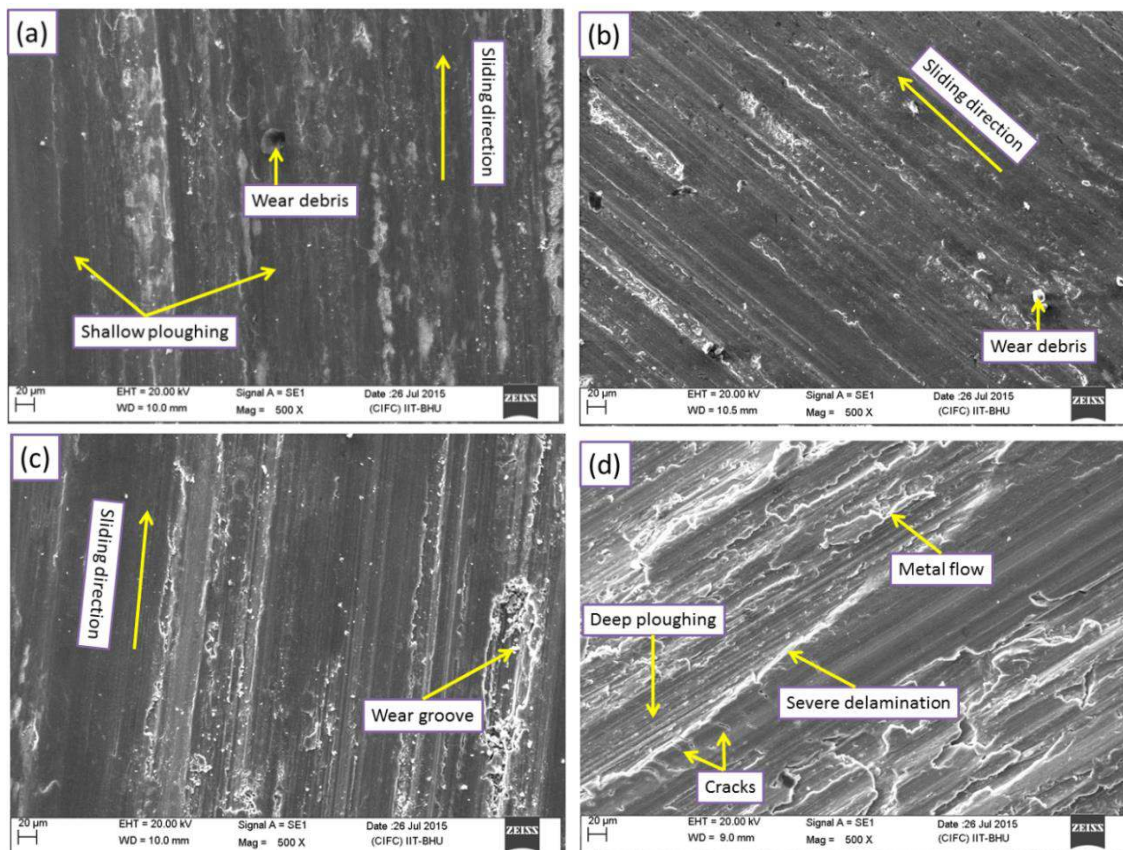


**Figure 4.17** - Worn surface morphology of 9 vol. % ZrB<sub>2</sub> composite at (a) 10 N (b) 20 N (c) 30 N and (d) 40 N load at 1 m/s sliding velocity and 6000 m sliding distance

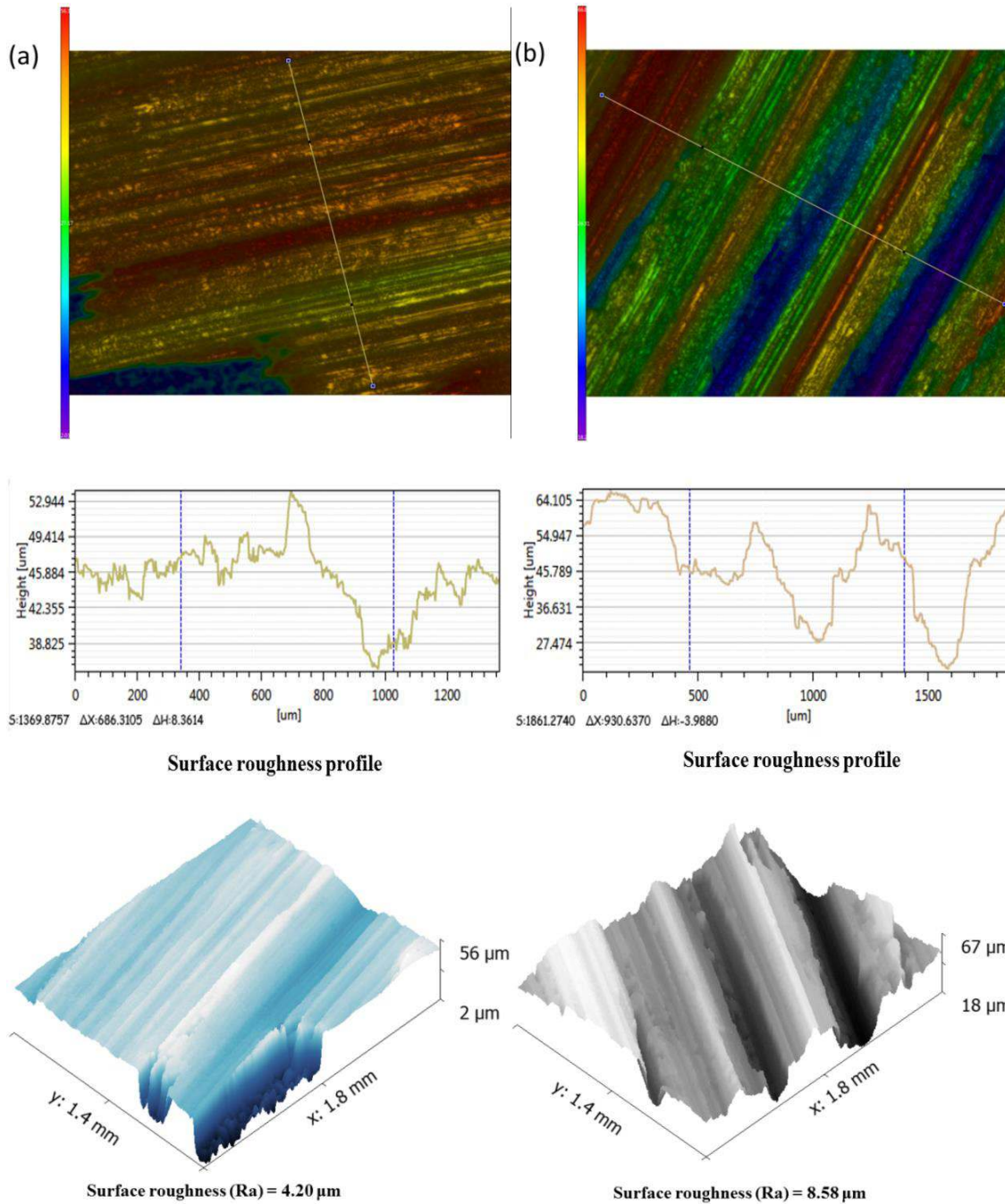


**Figure 4.18** - 2D and 3D topography of worn surface of 9 vol. % ZrB<sub>2</sub> composite at (a) 10 N and (b) 20 N load at 1 m/s sliding velocity and 6000 m sliding distance under profilometer

Figure 4.20a-d shows SEM micrographs of the worn surface at 20 N normal load and 1 m/s sliding velocity for AA5052 alloy and composites with 3, 6 and 9 vol. % ZrB<sub>2</sub>. Worn surface of matrix alloy (Fig.4.20a) exhibits deep grooves, large number of cracks, delamination and severely damaged areas which may be due the generation of high

frictional heating between the surfaces. Worn surface of composite (Fig.4.20d) shows shallow grooves, less delamination and damaged area. The wear debris is loose in nature and does not adhere to the surface due to hard  $ZrB_2$  particles. It is again clear from the worn surfaces that wear rate decreases when the content of  $ZrB_2$  particle increases.

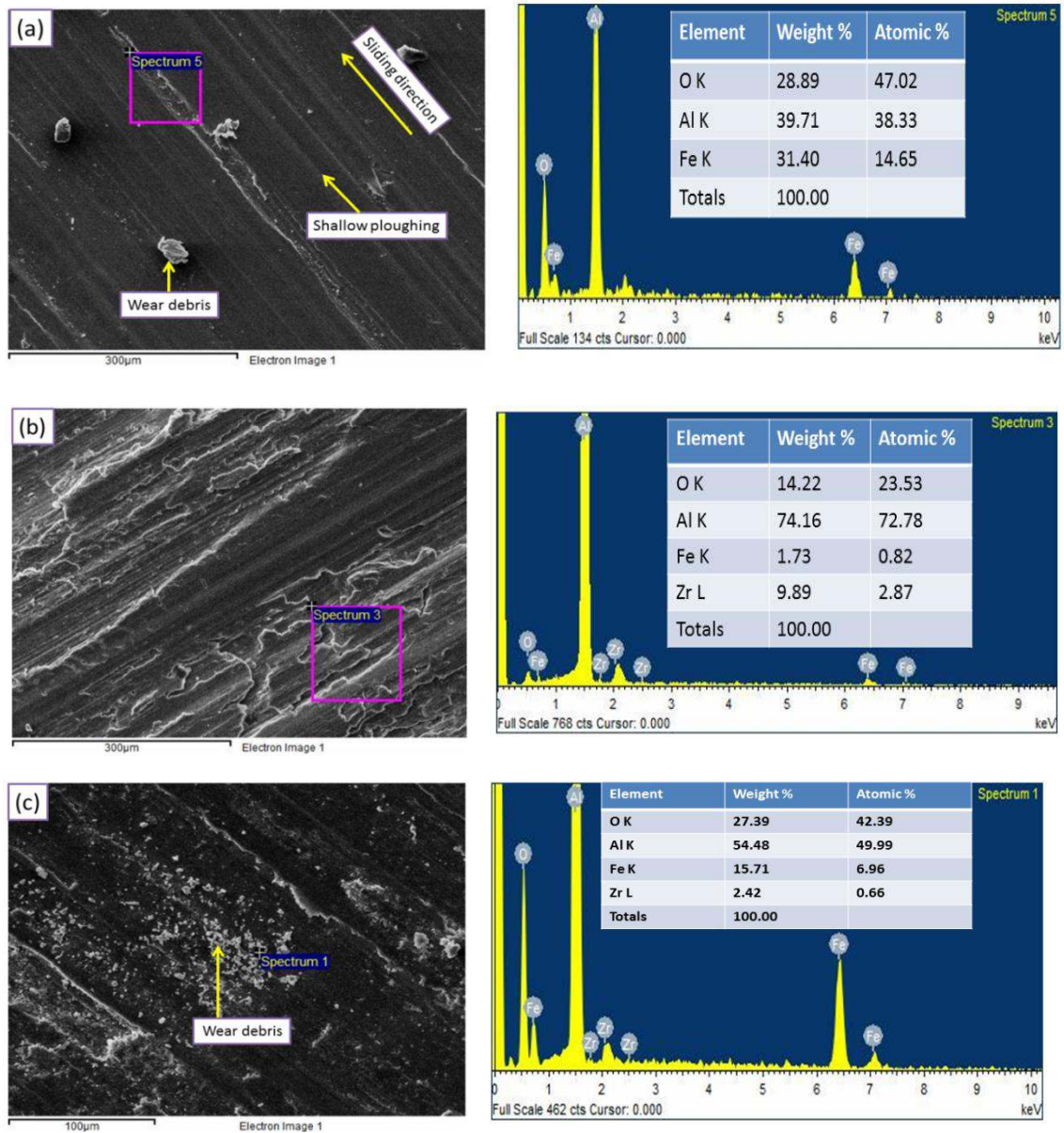


**Figure 4.19** - EDS pattern of 9 vol. %  $ZrB_2$  composite at (a) 10 N and (b) 40 N load (c) wear debris under 1 m/s sliding velocity and 6000 m sliding distance

Contour of worn surfaces in Fig. 4.21a-b shows different level of surface roughness and their profiles. 3D topography of worn surfaces also shows the deep ploughing grooves in AA5052 alloy as compared to the composite which exhibits shallow ploughing grooves (Fig.4.21a-b). The corresponding surface roughness values for base alloy and 9 vol. % ZrB<sub>2</sub> composite are 8.42 μm and 4.06 μm.

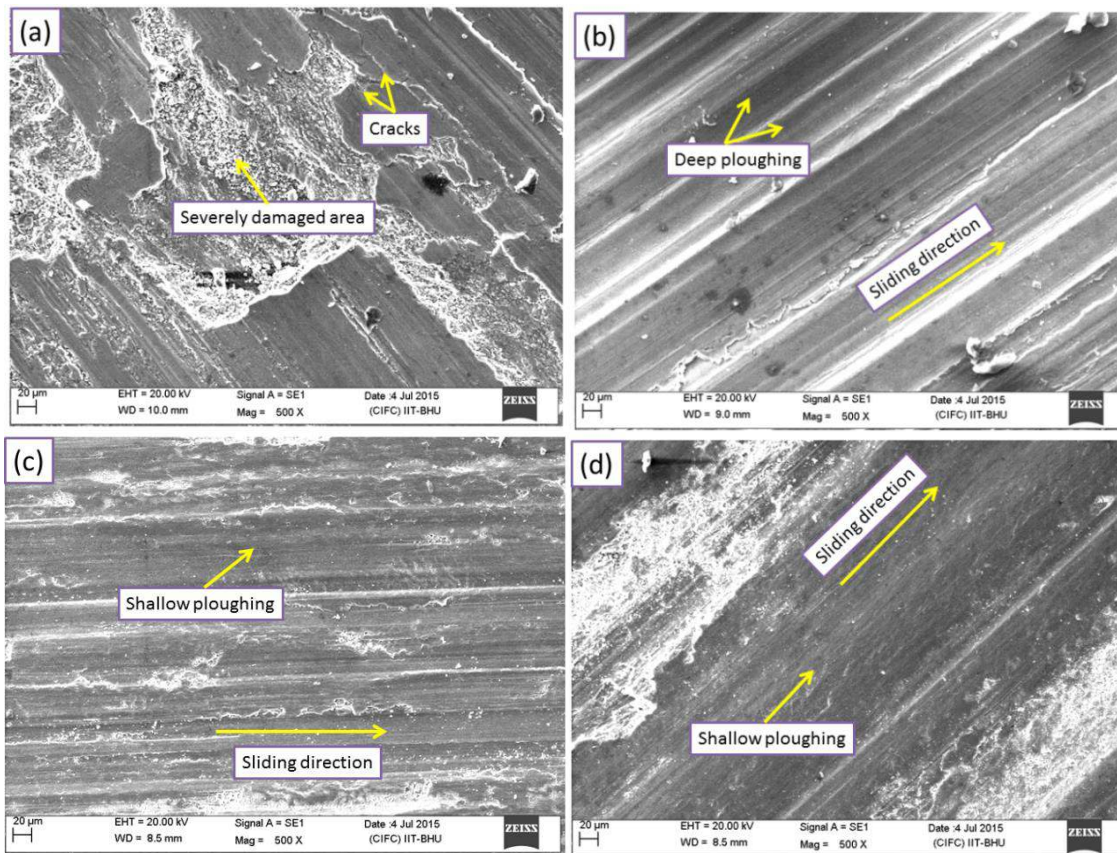


**Figure 4.20** - Worn surface morphology of (a) AA5052 alloy (b) 3 vol. % ZrB<sub>2</sub> (c) 6 vol. % ZrB<sub>2</sub> and (d) 9 vol. % ZrB<sub>2</sub> composite at 1 m/s sliding velocity and 6000 m sliding distance

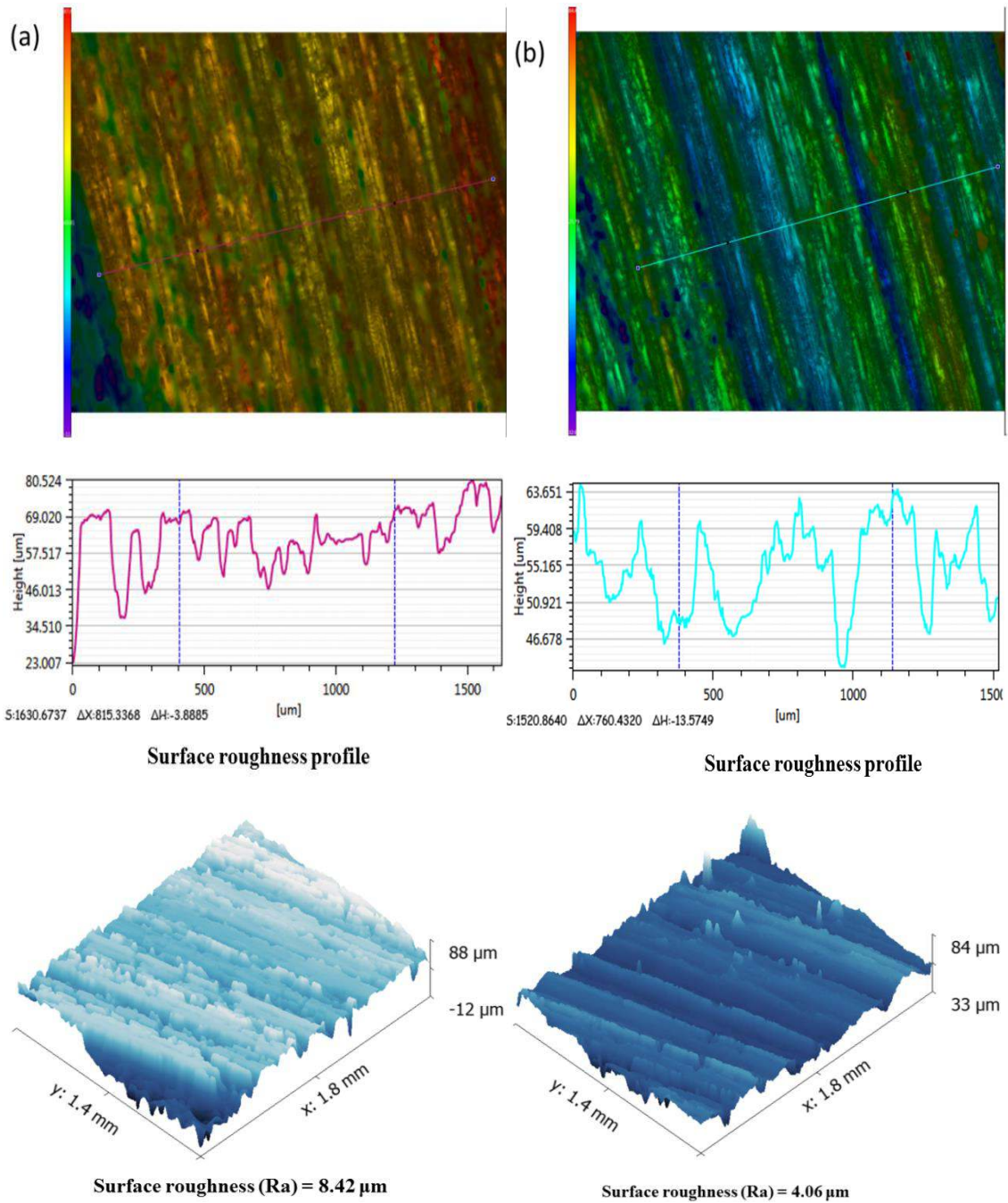


**Figure 4.21** - 2D and 3D topography of worn surface of (a) AA5052 alloy and (b) 9 vol. % ZrB<sub>2</sub> composite at 1 m/s sliding velocity and 20 N load after 6000 m sliding distance under profilometer

## 4.4 Conclusions

Following conclusions are drawn from the present chapter.

1. Wear rate, specific wear rate and normalized wear rate of composites decrease with increasing ZrB<sub>2</sub> content due to the increased hardness and grain refinement.

2. Wear rate with sliding velocity continuously increases.
3. Wear rate and wear rate per unit vol. % of  $ZrB_2$  particles increase with the normal load.
4. Coefficient of friction shows a fluctuating tendency with distance slid but with load it shows a decreasing trend up to 30N but beyond this load it increases sharply.
5. Coefficient of friction of composites increases with increase in  $ZrB_2$  particles and sliding velocity due to third body abrasion.
6. Wear track studied under SEM and Profilometer are in agreement with wear results. At low load and sliding velocity wear mode is mild-oxidative and it changes to severe- metallic at higher loads and sliding velocities.